Chemical Methodologies 7(2023) 307-313

Chemical Methodologies

Journal homepage: http://chemmethod.com

Original Research Article

Photodetector Biased on ZnO Nanoparticles/Poly-TPD Organic Material

Zahraa Hassan Ali*, **Lamees A. Abdullah**

University of Baghdad, College of Science, Department of Physics, Baghdad, Iraq

ARTICLE INFO

Article history

Submitted: 2022-11-01
Revised: 2022-12-04
Accepted: 2023-01-06
Manuscript ID: CHEMM-2301-1636
Checked for Plagiarism: Yes
Language Editor:
Dr. Fatimah Ramezani
Editor who approved publication:
Dr. Vahid Khakyzadeh

DOI:10.22034/CHEMM.2023.379131.1636

KEYWORDS

Zn
Structural Properties
Optical Properties
FE-SEM
Photodetector

ABSTRACT

In the present study, a photodetector was prepared by depositing PEDO TPSS and TPD polymer on porous silicon (PSi) substrates using spin coating technique. The response time of the manufactured PSi/PEDOTPSS/TPD detector (by illuminating the sample with a 250 W/cm^2 tungsten lamp) was 8.83s and measured in the second scale. The detection, specific detectivity, and responsivity of the both detectors were found as 3.395x10^{9}W^{-1}, 1.967x10^9 W^{-1} Hz$^{1/2}$ cm and 5.188x10^{-3} A/W, respectively. The incorporation of ZnO nanoparticles with a TPD polymer improved the detection, specific detectivity, optical response, and detector response time to 74.62x10^9 W^{-1}, 43.25x10^9 W^{-1} Hz $^{1/2}$ cm ,1893.16x10^{-3} A/W, and 1.06066 s, respectively. The Hall Effect measurements revealed that the n-type nanoparticles have the carrier concentration around -3.90×10^{17} cm^{-3}.

GRAPHICAL ABSTRACT

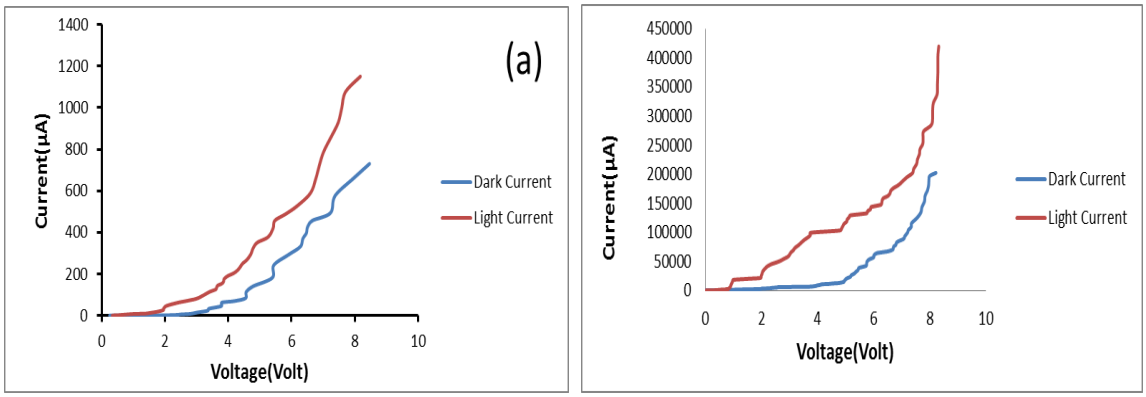

* Corresponding author: Zahraa Hassan Ali
✉ E-mail: zahraa.hasan1204a@sc.uobaghdad.edu.iq

Introduction

Since nanoparticles contain a considerably higher number of surface atoms than bulk materials, II-VI nanocrystal line semiconductor materials have been the subject of intense researches [1]. Many physical properties of nanostructure semiconductors depend strongly on their size, shape, and crystal structure. Because of their very small size, nanostructures exhibit different optoelectronic behaviours than bulk semiconductors of the same composition [2].

A photodetector is a device that frequently employs a semiconductor with a specific bandgap, wherein arriving photons with a sufficient energy will excite electrons in the valence band to the conduction band, producing an electron that is mobile and leaving a hole within the valence band. The resulting current is observable because the produced charge-hole pairs will react to a bias in a manner similar to that of a conductor. These charge-hole couples will recombine and produce heat for a finite amount of time [3]. Amongst the known semiconductor substances, zinc oxide (ZnO) is one of the more alluring options due to its high exciton binding energy of 60 meV, wide bandgap energy of 3.37 eV at ambient temperature, exceptional chemistry, thermal stability, and biocompatibility [4, 5].

The common N′-diphenylbenzidine, conductive polymer TPD (alkyl-TPD), possesses a 5.5 eV ionization potential and an excellent transport hole mobility of 10^3 cm^2/Vs [6, 7]. TPD typically serves as the host material or a blue-violet light emitting material on phosphorescence organic light emitting diodes because of its wide energy band of about 3.2 eV with the highest occupied molecular orbital (HOMO) and the lowest unoccupied molecular orbital (LUMO) energies of 5.5 eV and 2.3 eV, respectively [8]. For UV detection, a porous silicon photodetector is typically utilized porous silicon photodetector, which has numerous privileges on other materials, including a high UV absorption coefficient, low cost, and ease of production [9, 10].

PEDOT:PSS, also known as poly (3,4-ethylenedioxythiophene) polystyrene sulfonate, is a combination of two ionomers. One of the components of this mixture is sodium polystyrene sulfonate. A part of the sulfonyl groups is negatively charged and deprotonated. The other component is a conjugated polymer with positive charges based on polythiophene called poly(3,4-ethylenedioxythiophene) (PEDOT). When the charged macromolecules come together, a macromolecular salt is produced [11]. Ethylene dioxythiophene monomer is used to create PEDOT, a polymer. Electrical conductivity of the substance is influenced by delocalized π-electrons within its chemical structure with the presence of sulfonated polystyrene (PSS). The monomer has many advantages such as its mechanical properties of (E≈1.2 GPa), optical properties of T>90%, and electronic and ionic conduction [12].

In this study, more than one detector was manufactured to improve the optical response of the visible detectors. In all the manufactured photodetectors, PSi was used as a substrate.

Materials and Methods

The zinc oxide was prepared by pulsed laser ablation method. Nd:YAG laser was utilized in the deformation process. The laser is working with a frequency of 6 Hz, wavelength of 1064 nm, power of 1000 mJ with 4000 pulses, and pulse period of 7 ns. The laser pulses were directed at a 2 mm of ZnO dry bulk sample submerged in chloroform.

The TPD solution was created by blending 3 mL of chloroform with 0.075 g of TPD and stirred until a dissolution process was complete.

Silicon of n-type (n-Si) with a cross section area of 1.5×1.5 cm^2 and resistivity of (0.008-0.02) Ω.cm was utilized in this study. In Teflon etching cell, the Si substrate was inserted in a solution of aqueous hydrogen fluoride of a purity of 40% and ethanol of purity of 99.99% at 1:1 volume ratio. This method was used to create the n-PSi layers. The sample was anodized using 20 mA/cm^2 current density for 20-min etching period. To prevent oxidation, the sample was cleaned with

ethanol after the etching procedure and kept in a glass container.

The fabrication of photodetector device was started by depositing PEDOT PSS on PSi substrate at a speed of 1500 rpm for 30 s. Then, the PSi/PEDOT PSS was put for 20 min in an oven at 120 °C to be matched with the substrate. After that, the p-TPD was deposited by spin coating method to obtain the detector. The TPD was deposited on PSi/PEDOT PSS at 3000 rpm for 30 s. After the deposition process, the sample was heated to 50 °C in an oven for 30 min to finish the drying. The aluminium electrodes were deposited by thermal evaporation technique.

Another photodetector was manufactured and the P-TPD polymer was utilized by combining it with ZnO NPs to create the photodetector sensitive active layer. The mixture was deposited on the PSi/PEDOT PSS. The detector sensitive area was set up as follows:

The TPD solution was created by blending 3 mL of chloroform with 0.075 g of TPD and stirred until a dissolution process was completed.

The ZnO solution was created by blending 3 mL of chloroform with 0.02 mL of zinc oxide and stirred until a dissolution process was completed.

To create the PSi/PEDOT PSS/TPD:ZnO enhanced detector, the ZnO-chloroform solution and TPD-chloroform solution were mixed in a mole ratio of 2:1 before being deposited on the PSi/PEDOT PSS by the spin coating method, and then the sample was heated to 50 °C in an the oven for 30 min to finish the drying.

Results and Discussion

Morphological properties

The images obtained by a scanning electron microscope are displayed in Figure 1, which creates images of a sample surface at high fidelity. It shows size, shape, and crystal structure for the ZnO NPs which were detected as spherically clustered and bright spots with average particle sizes of 57-67 nm.

Optical properties of ZnO nanoparticles

The measurements of UV-Vis, photoluminescence (PL), were used to determine the optical characteristics of the ZnO nanoparticles. The absorbance spectra showed wavelength dependency in the 290-1090 nm region. The semiconductor optical energy band gap (Eg) was derived from the Tauc equation [13], as shown in Figure 2.

The film's absorbance was quite high in the UV region and it decreased exponentially with wavelength. This suggests that ZnO NPs have high responsiveness in the UV region [14]. As the chart of $(\alpha h\nu)^2$ against $(h\nu)$ reveals an intermediate linear area, linear extrapolation portion can be used to determine Eg from the intersection with the $(h\nu)$ axis, as depicted in Figure 3.

The calculated Eg for ZnO was about 3.05 eV. Figure 4 displays the photoluminescence spectrum for the zinc oxide nanoparticles. The sample was excited with a source with a wavelength of 310 nm. The first peak was centred at 407 nm and correlated with native deep defect levels for nanoparticles where were linked to the movement from VZn to Zni or from VZn to C.B. The second peak was centred at 622 nm, which was referred to the second-harmonic generation.

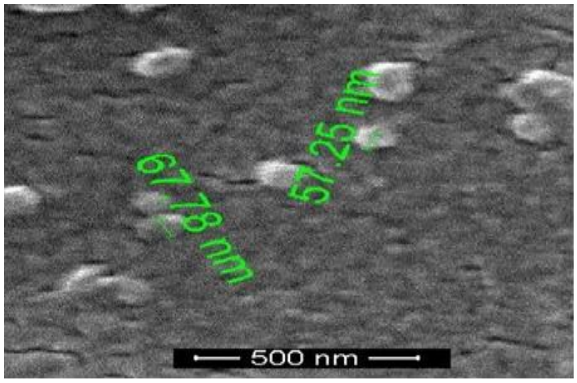

Figure 1: The SEM images of ZnO NPs

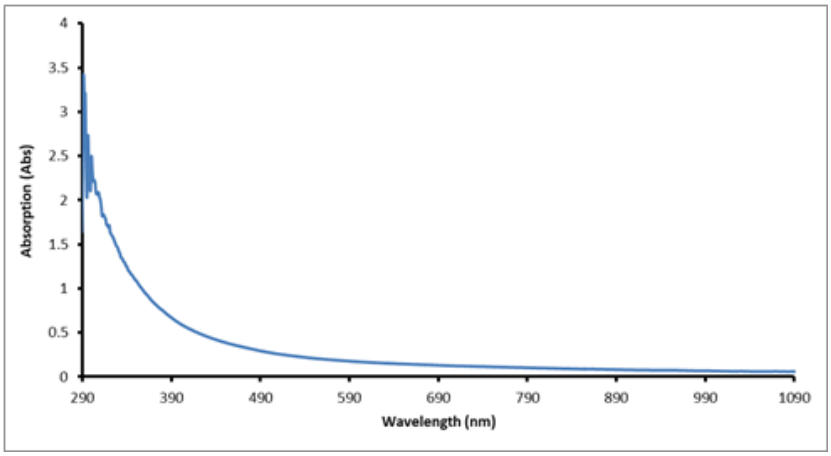

Figure 2: The absorption spectrum of ZnO NPs

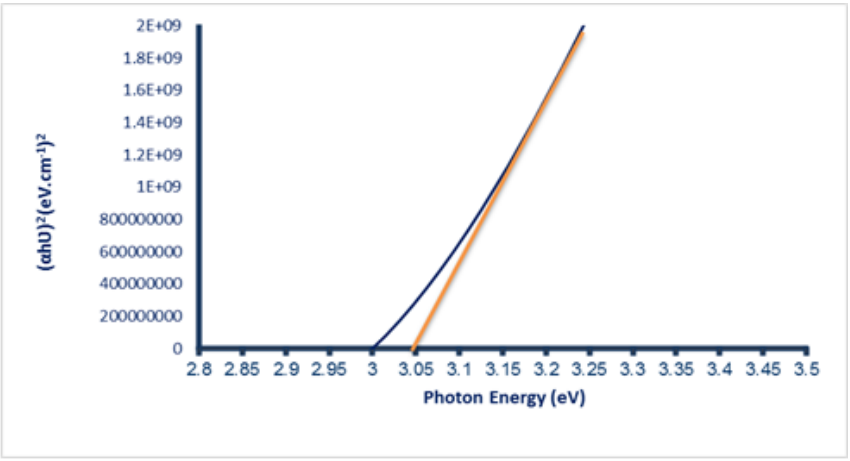

Figure 3: $(\alpha hv)^2$ vs. photon energy of the ZnO NPs

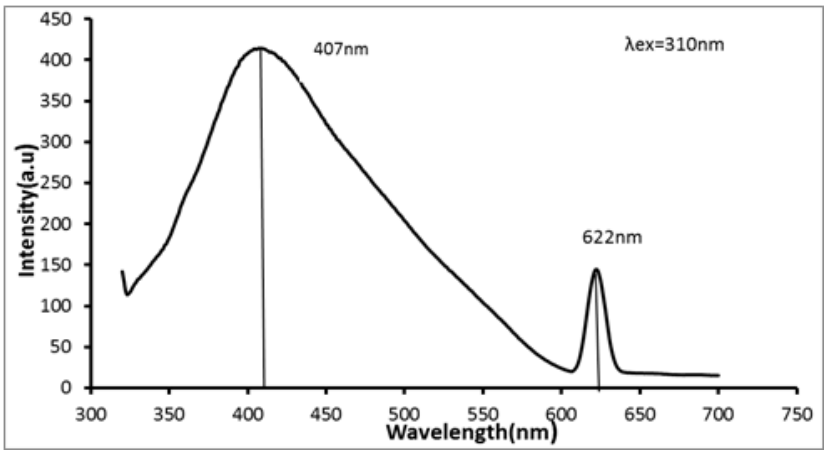

Figure 4: The photoluminescence spectrum of the ZnO NPs at λext of 310nm

Electrical properties of ZnO nanoparticles

Hall effect

The electrical properties of the ZnO NPs were studied using Hall Effect setting type (HMS3000). The film displays the behaviour of n-type conductivity, resistivity, and mobility which were 2.55×10^{1} $(\Omega.cm)^{-1}$, 3.92×10^{-2} $(\Omega.cm)$ and 4.09×10^{2} $(cm^2/V.sec)$, respectively. The carrier concentration was -3.9×10^{17} cm^{-3}, and the Hall coefficient was -1.6×10^{1} $(1/cm^3.C)$.

Current–voltage (I-V) measurements

The current-voltage characteristics of the photodetector were examined at dark and under illumination of 250 W of tungsten halogen light. There was an increase in the current was observed at room temperature. The I-V characteristics of the PSi/PEDOT PSS/TPD:ZnO and PSi/PEDOT PSS/TPD photodetectors are depicted in Figure 5. The most used method for characterizing devices is the current-voltage curves. The current densities for the both detectors were 1.297 and 473.29 A/cm^2, respectively.

The increase in the photocurrent of the coated PEDOT PSS/TPD:ZnO detector Psi specimens was much higher than that of the photocurrent of the coated PEDOT PSS/TPD detector Psi samples.

The photoconductive gain (G) is determined by the ratio of the photocurrent to the dark current for a same voltage applied is given by the relationship; $G = \tau / T$, where τ is the charge carries life time and T is the transit time between the detector electrodes. The photocurrent gain of the PSi/PEDOT PSS/TPD detector was 1.57, while that of the PSi/TPD:ZnO detector was 2.07. Using the values of photocurrent gain and the transit time of the detectors, the carry life times were determined of about 27.475 and 3.105 s for PSi/PEDOT PSS/TP and PSi/PEDOT PSS/TPD:ZnO detectors, respectively.

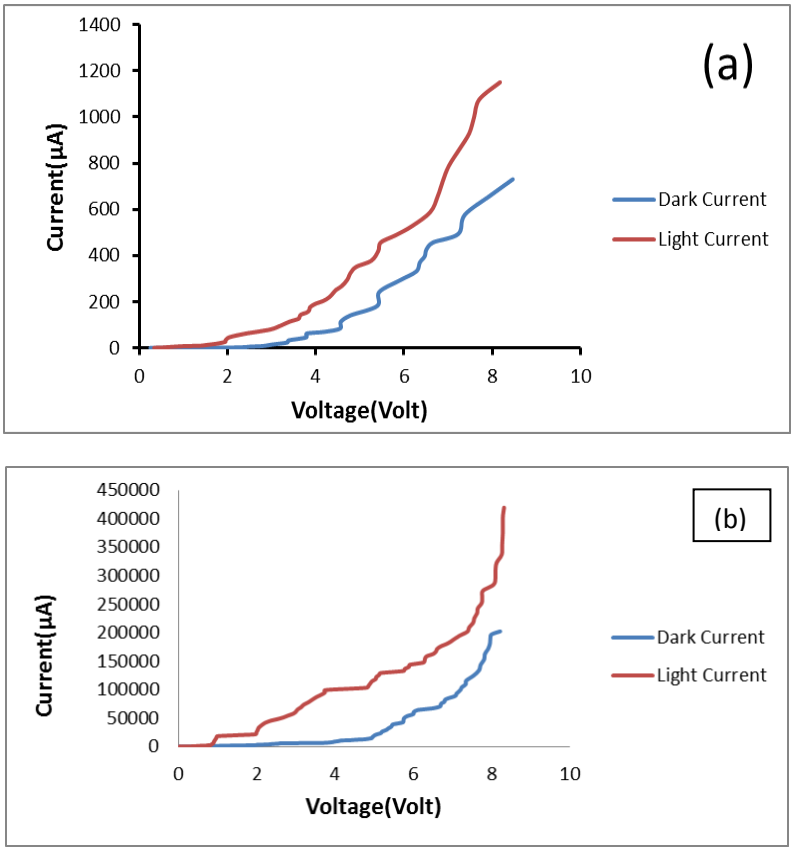

Figure 5: I–V measurements of (a) PSi/PEDOTPSS/TPD photodetector. (b) PSi/PEDOTPSS/TPD: ZnO photodetector

The transit time is associated to the electrode spacing and the carries mobility which is given by the relationship: $T = L^2/\mu V$, where L is the electrode spacing, μ is the carry mobility and V is the bias voltage. Using the values of carries mobility, the transit time was 8.3117×10^{-6} and 96.9697×10^{-6} (cm^2/v.sec) for each detector, respectively.

The specific detectivity D*, also known as the normalized detectivity, is the reciprocal of the noise equivalent power (NEP) which was normalized to the detector area of 0.336 cm^2 and the noise electrical band width f of 1 Hz. It can be represented as follows [15]:

$$D^* = R_\lambda (A\Delta f)^{1/2} / I_n \quad (1)$$

Where, A is the detector sensitivity area, R_λ is the optical response of the photodetector in (A/W), and I_n is the noise current which can be calculated from dark current using the following relationship [16]:

$$I_n = (2eI_d \Delta f)^{1/2} \quad (2)$$

Where, e is the electronic charge, Δf is the noise bandwidth, and I_d is the dark current which is resulting in a noise current. The noise current for PSi/PEDOTPSS/TPD and PSi/PEDOTPSS/TPD:ZnO detectors was 1.528×10^{-11} and 25.449×10^{-11}A, respectively, at Δf =1 Hz. Using the value of optical response and A=0.0008865 cm^2, the specific detectivity for PSI/ PEDOT PSS/TPD and PSI/PEDOT PSS /TPD: ZnO detectors was 1.967×10^9 and 43.25×10^9 W^{-1} $Hz^{1/2}$ cm, respectively.

This study was clearly demonstrated the process of the production of ZnO thin films. The accompanying graphs of the ZnO particle dynamics illustrated this film. They showed signs of H_2S with improved sensitivity, faster response, and slower recovery time of the sensors. The hydrothermal method is the best method for preparing zinc oxide because it contains no by-products, economically feasible, and does not produce fumes or toxic substances that are difficult to remove. It was also showed that increasing the reaction time by no more than 2 hours leads to an increase in the incident rays in the longest UV wavelength range. It can be concluded that the large increase in the energy gap was due to the effect of the quantum size, and the amount of the energy gap qualifies the material to be a large effective medium in ultraviolet photodetectors. The FSEM results demonstrated that the surface has a nanostructure and that nanoparticles of average size were present.

Conclusion

In this study, the photoconductive detector was fabricated using two types of PEDOT PSS, TPD polymers and deposited on porous silicon (PSi) by spin coating method. The ZnO was incorporated into the TPD polymer and was significantly improved the photoconductive gain from 1.57 to 2.07. By adding ZnO nanoparticles, the responsivity was increased from 5.188×10^{-3} to 1893.16×10^{-3} (A/W), and the time response was decreased from sec. The obtained results were compared with previous works and found to be close to them [17-19].

Funding

This research did not receive any specific grant from funding agencies in the public, commercial, or not-for-profit sectors.

Authors' contributions

All authors contributed to data analysis, drafting, and revising of the paper and agreed to be responsible for all the aspects of this work.

Conflict of Interest

We have no conflicts of interest to disclose.

Orcid

Zahraa Hassan Ali
https://orcid.org/0000-0002-6471-1034
Lamees A. Abdullah
https://orcid.org/0000-0002-0778-7411

References

[1]. Elilarassi R., Maheshwari S., Chandrasekaran G., Structural and optical characterization of CdS nanoparticles synthesized using a simple chemical reaction route. *Optoelectron. Adv. Mater. Rapid Commun*., 2010, **4**:309 [Google scholar], [Publisher]

[2]. Fu Y., Qiu M., Optical Properties of Nanostructures, 1st Ed, Pan Stanford, 2011, p 312 [Crossref], [Publisher]

[3]. Alaie Z., Nejad S.M., Yousefi M.H., Recent advances in ultraviolet photodetectors, *Materials Science in Semiconductor Processing,* 2015, **29**:16 [Crossref], [Google scholar], [Publisher]

[4]. Chen J., Zhang Y., Skromme B. J., Akimoto K., Pachuta S.J., Properties of the shallow O-related acceptor level in ZnSe, *Journal of Applied Physics*, 1995, **78**:5109 [Crossref], [Google scholar], [Publisher].

[5]. Kato H., Sano M., Miyamoto K., Yao T., Homoepitaxial growth of high-quality Zn-polar ZnO films by plasma-assisted molecular beam epitaxy, *Japanese journal of applied physics*, 2003, **42**:L1002 [Crossref], [Google scholar], [Publisher]

[6]. Chilton J.A., Goosey M.T., C. CHEM. FRSC, FIM.: *Special polymer for electronics and optoelectronics*, 1995, p 351. [Crossref], [Publisher]

[7]. Csavinszky P., Quantum Mechanical Treatment of Transport Properties of Semiconductors: Possible Application to Polymers, In *Quantum Theory of Polymers*, Springer, Dordrecht, 1978, **39**:289 [Crossref], [Google scholar], [Publisher]

[8]. Wang F., Chen Z., Xiao L., Qu B., Gong Q., Enhancement of the power conversion efficiency by expanding the absorption spectrum with fluorescence layers, *Optics Express.*, 2011, **19**:A361 [Crossref], [Google scholar], [Publisher]

[9]. Berger M.G., Dieker C., Thonissen M., Vescan L., Luth H., Munder H., Theiss W., Wernke M., Grosse P., Porosity superlattices: a new class of Si heterostructures. *J Phys D Appl Phys*, 1994, **27**:1333 [Crossref], [Google scholar], [Publisher]

[10]. Ismail R.A., Fabrication and Characterization of Photodetector Based on Porous Silicon. *J Surf Sci Nanotechnol*. 2010, **8**:388 [Crossref], [Google scholar], [Publisher]

[11]. Groenendaal L., Jonas F., Freitag D., Pielartzik H., Reynolds J.R.., Poly (3, 4-ethylenedioxythiophene) and its derivatives: past, present, and future, *Advanced materials*, 2000, **12**:481 [Crossref], [Google scholar], [Publisher]

[12]. Jenny Nelson, Photovoltaic Effect: An Introduction to Solar Cells, The physics of Solar Cells, *Imperial College Press*, 2003

[13]. Tauc J., Optical properties and electronic structure of amorphous Ge and Si, "Materials Research Bulletin," 1968**, 3**:37 [Crossref], [Google scholar], [Publisher]

[14]. Pankove J.I., Optical processes in semiconductors Prentice-Hall, *New Jersey*, 1971, **92**:36 [Google scholar]

[15]. Samnely, Y.Liao, Microwave Solid-State Devices, Ch.9, 1983, p 11. [Publisher]

[16]. Nasir E.M., "Fabrication of CdSe: Cu Photoconductive Detector by using Vacuum Evaporation Technique and studying its Electro-Optical Properties", M.Sc. Thesis, University of Baghdad, Dep. f Physics, 1999 [Google scholar]

[17]. Dai R., Liu Y., Wu J., Wan P., Zhu X., Kan C., Jiang M., Self-powered ultraviolet photodetector based on an n-ZnO: Ga microwire/p-Si heterojunction with the performance enhanced by a pyro-phototronic effect, *Optics Express*, 2021, **29**:30244 [Crossref], [Google scholar], [Publisher]

[18]. Wan P., Jiang M., Xu T., Liu Y., Kan C., High-mobility induced high-performance self-powered ultraviolet photodetector based on single ZnO microwire/PEDOT: PSS heterojunction via slight ga-doping, *Journal of Materials Science & Technology*, 2021, **93**:33 [Crossref], [Google scholar], [Publisher]

[19]. Muhammad A., Mohammad S.M., Hassan Z., Rajamanickam S., Abed S.M., Ashiq M.G.B., Fabrication of fluorine and silver co-doped ZnO photodetector using modified hydrothermal method, *Microelectronics International*, 2022, **40:1** [Crossref], [Google scholar], [Publisher]

HOW TO CITE THIS ARTICLE
Zahraa Hassan Ali, Lamees A. Abdullah. Photodetector Biased on ZnO Nanoparticles/Poly-TPD Organic Material. *Chem. Methodol.*, 2023, 7(4) 307-313
https://doi.org/10.22034/CHEMM.2023.379131.1636
URL: http://www.chemmethod.com/article_164843.html